Research Article GU J Sci 36(2): 555-571 (2023) DOI: 10.35378/gujs.1047479

Gazi University

Journal of Science

http://dergipark.gov.tr/gujs

Free Vibration Response of a Steel Liquid Storage Tank with Porous and Perforated Columns via an Exact Continuum Method

Togay KUPELI*, Yakup Harun CAVUS, Busra UZUN, Mustafa Ozgur YAYLI

Bursa Uludag University, Faculty of Civil Engineering, 16059, Bursa, Turkey

Highlights

- This paper focuses on vibrational responses of steel liquid storage tanks.
- An exact continuum method is proposed for calculation of vibrational frequencies of storage tanks.
- A highly efficient method is proposed for free vibration of storage tanks under various effects.

Article Info

Received: 26 Dec 2021
Accepted: 22 May 2022

Keywords

Storage tank
Porosity
Perforated column
Stokes' transform
Continuum model

Abstract

The presence of predictable cavities inside a structure is often preferable as it will reduce the vibration amplitude. In this article, inspired by the traditional mass attached to the beam system, in order to solve the problem of free vibration of the steel liquid storage tank with a column made of porous and perforated materials using an exact analytical continuum model is formed. The free vibration response of the mass attached column made of porous materials and holes is established by using a new analytical method known as the Fourier series with Stokes' transform. The free vibration frequencies are obtained by using an eigen-value approximation, and the influences of the number of holes, filling ratio, porosity and other parameters on the free vibration response are explored. It is shown that an increase in the mass parameter, filling ratio and porosity parameter of the column with an attached mass system could significantly affect the free vibration response of the system.

1. INTRODUCTION

Many studies on the term porosity can be found in the literature. The topic of porosity in relation to columns received a lot of attention in these researches. Many different types of studies on porosity in structural and mechanical aspects, as well as porosity in multiple sectors can be found in the literature. Kirkland [1] examined the controlled surface porosity column packings. As a result of this investigation, the relationship between speed and porosity on the surface was analyzed. To determine the exterior porosity of compacted and solid reversed-phase columns. Cabooter et al. [2] searched total pore blockage as an alternate way. They introduced a new method for determining the interfacial void capacity. Alyousef et al. [3] designed a model to establish the porosity of concrete as an essential mechanical feature. In a numerical analysis of Alyousef et al.'s work, it showed the porosity parameters and the intensity of interactions with hazardous substances. Huang et al. [4] examined the effect of porosity and cement grade on the mechanical properties of concrete. Using a revised trigonometric shear deformation model to study the mechanical properties of porous FG (Functionally Graded) plates conducted by Bekkaye et al. [5]. Deflection and buckling analysis of porous FG plates under mechanical strain were the main topics of Bekkaye's work. Many articles were written about the terms "porosity" and "strength". These topics were worked on by Gouda, Roy [6], and Erniati et al. [7]. Kim, Edil and Park [8] tested porosity and flowrate in a column of compacted clay. The aims of this article, which was published by Kim, Edil and Park are to quantify effective porosity using a tracer test and compare it to total porosity calculated using phase relationships and weight/volume measurements. Sousa et al. [9] presented the content of high-porosity nanostructured polymer modular microfluidic columns for biochemical research. Their objective is to achieve high-speed and high-resolution gradient separations of intact biomolecules targeted at high-speed and high-resolution microfluidic devices. Many articles also discussed beams and porosity terms together. As an example, analyzing the impact of

*Corresponding author, e-mail: togay-kupeli@hotmail.com

powder and post-processing on porosity and characteristics of electron beam melted Ti-6Al-4V was published by Cunningham et al. [10]. Exploration on solutions for torsion vibration of a porous nanostructure was also investigated by Najafzadeh et al. [11].

A storage tank that have designed is included in the material of this paper. The Housner approach is one of several different seismic design procedures for storage tanks. Eurocode 8 and ACI 350 are two of the most major design standards. This design process and its criteria have been extensively studied in the literature. Sloshing and fluctuation reduction of the water storage tank of AP1000 (AP1000 is a standard design developed by Westinghouse for an advanced generation III+ nuclear power plant (NPP) utilizing passive features) were investigated by Zhao et al. [12]. The main aim of this research is to evaluate the impacts of fluid–structure interaction (FSI) on the dynamic performance of a water tank and the impacts of water sloshing on the shield building's seismic response numerically. Kim and Lee [13] published the other paper containing vibration analysis on storage tanks. In Kim and Lee's study, the vibration characteristics of the sloshing and bulging modes for a liquid-filled rigid circular cylindrical storage tank with an elastic annular plate in contact with the sloshing surface of liquid were investigated using an analytical technique. Cho et al. [14] and Tedesco et al. [15] presented publications on structural analysis and free vibration in storage tanks. The content of the papers includes vibration frequency analyses and structural modifications for storage tanks.

Perforated material may be utilized in innovative architectural applications such as archways, facades, platforms, and panels, and its properties provide for inventiveness with light, sound, and visual dimension. Perforated metal can be used to control light and ventilation within a space. There are some advantages to using perforated material, as has been used in this study. An example of this can be easily observed that employing oversized isolated holes is an efficient method of optimizing connection behavior by boosting ductility, rotational performance, and energy dissipation capacity. There are studies in the literature on perforated columns, which are also discussed in this study. Pina and Meirelles [16] examined the deacidification of maize oil using a rotating disc column and continuous liquid-liquid extraction. Tsavdaridis et al. [17] published work about fully fixed (welded) perforated beam-to-column connections applied as seismic-resistant design strengthening approaches. The efficacy of broadband low-frequency sound absorption through graduated perforated porous materials backed by Helmholtz resonant cavities was examined by Liu et al. [18]. There are also articles in the literature in which vibration analyses and calculations were made using perforated materials [19-21].

In recent articles, it is seen that various solution methods, as in the generalized technique of differentiable quadrature, the Navier solution, separation of variables, the Ritz method, Stokes' transform, Fourier series, and the finite element method, attract attention. Previous studies in the literature provided examples of these methods [22–35]. Various studies on free vibration analysis, one of the main subjects of our research, are also regularly featured in the literature. Karabulut and Ersoy studied a two-cylinder, four-stroke internal combustion engine's vibrational characteristics [36]. The free vibration study of a functionally graded (FG) micro-beam with a conical cross-section was performed by Ipci and Yildirim [37]. One of the most productive studies in the field of buckling and vibration is the study of nonlinear theories for deflection, buckling and vibration of beams published by Reddy [38].

In this research article, the design of a water tank has been created with the use of a porosity column in order to partially differentiate this study. Within the scope of the study, in addition to porosity, analysis has been performed with perforated. The pre-sizing of the porous and perforated columns and the design of the storage tank been completed as part of this study. In this research, a new analytical method called the Fourier series with Stokes transform has been used to determine the free vibration response of the column containing a load and spring attached to its end. The column of the storage tank has been modeled with two different materials: porous and perforated. Once the design phase of the water tank has been prepared, vibration frequency analyses based on various parameters have been performed. These parameters are number of holes, filling ratio, e_1 porosity parameter, e_2 porosity parameter, mass and spring parameters. The study's tables and figures have been presented in an illustrative manner to demonstrate how the vibration frequency values change when the variable parameters have changed.

2. MATERIAL and METHOD

In this section, a technique of analysis has been proposed that can calculate the vibration frequencies of storage tanks (Figure 1). The water tank is modeled in a form carried on columns with porous and perforated sections as in Figure 2. In addition, a horizontally directed spring is used to prevent the vibration amplitude from being too high. As it is known, most of the studies in the literature use the lumped mass model, in which the storey masses are considered infinitely rigid.

Figure 1. *A storage tank made of steel material*

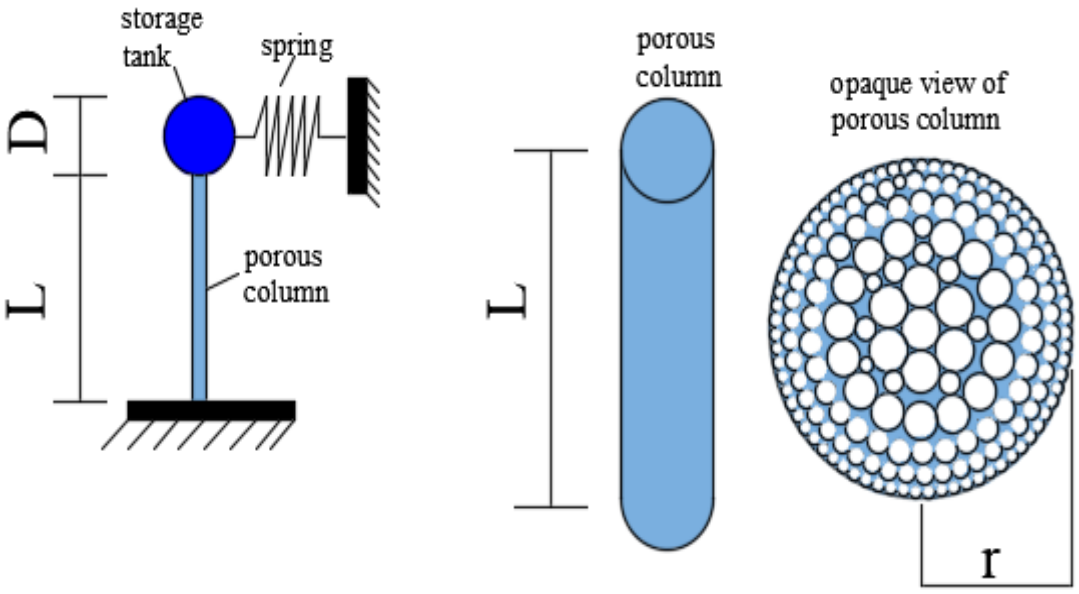

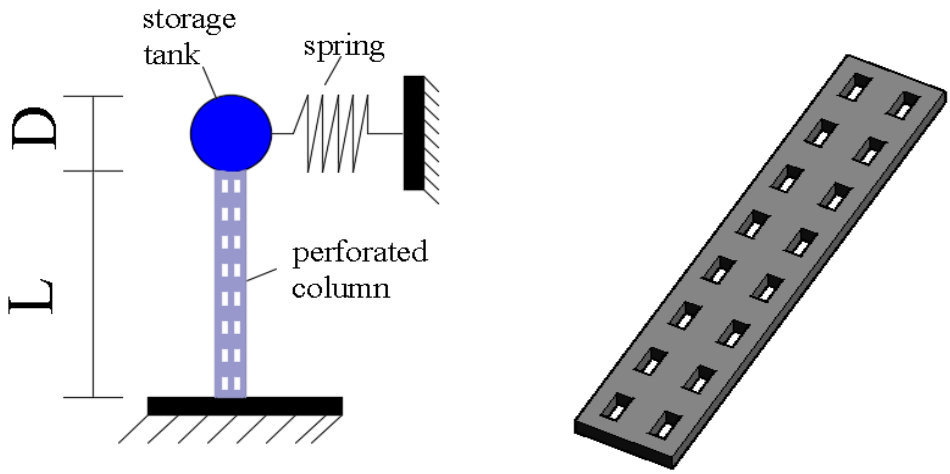

Figure 2. *The storage tank's idealized models and opaque views of porous and perforated column*

2.1. Formulations

It has been said before that this work is inspired by a cantilever classical beam with a mass and spring added to its end. In the first part of this study, studies [34–35, 38] using various beam theories are mentioned. These references take into account various effects, such as size effects, and when these effects are neglected in their formulation, the vibration equation of a column based on Euler-Bernoullli beam theory is written as:

$$EI\frac{\partial^4 w(x,t)}{\partial x^4}+\rho A\frac{\partial^2 w(x,t)}{\partial t^2}=0 \tag{1}$$

where E is the Young's modulus, I denotes the inertia moment, ρ represents the material's mass density and A specifies of the cross-sectional area. Also, $w(x,t)$ represents the lateral displacement used to describe the lateral vibration of the column. In this study, the dynamic behavior of the storage tank when the column consists of porous and perforated material is presented and compared with each other. The Young's modulus and the mass density of the column, which is considered to have a porous circular section, are defined by the formulas given below [11]:

$$E(r)=E_o(1-e_1\cos(\frac{\pi r}{2R})) \tag{2}$$

$$\rho(r)=\rho_o(1-e_2\cos(\frac{\pi r}{2R}))\,. \tag{3}$$

In these equations, R indicates the radius of the porous column, while E_o and ρ_o symbolize the Young's modulus and mass density properties in the outer radius of the column, respectively. e_1 and e_2 represent the porosity originating from the Young's modulus and mass density, respectively. They may be expressed as follows [11]:

$$e_1=(1-\frac{E_i}{E_o}) \tag{4}$$

$$e_2=(1-\frac{\rho_i}{\rho_o}) \tag{5}$$

where E_i and ρ_i are the Young's modulus and mass density properties in the center of the column, respectively. Bending stiffness specified with EI in Equation (1) can be written for porous column as *E(r)I*. Similarly, mass per unit length ρA may be rewritten for porous columns as $\rho(r)A$. Another situation considered for the column to be analyzed is the perforated section. To accomplish the investigation of the perforated column, equivalent bending stiffness $(EI)_{eq}$ and mass per unit length $(\rho A)_{eq}$ should be calculated. Bending stiffness and mass density per unit of column with perforated section are given by Abdelrahman et al. [27] as follows:

$$\left(EI\right)_{eq} = EI\,\frac{\alpha(N+1)(N^2+2N+\alpha^2)}{(1-\alpha^2+\alpha^3)N^3+3\alpha N^2+(3+2\alpha-3\alpha^2+\alpha^3)\alpha^2 N+\alpha^3} \tag{6}$$

$$\left(\rho A\right)_{eq} = \rho A\frac{[1-N(\alpha-2)]\alpha}{N+\alpha} \tag{7}$$

where N represents the number of holes throughout the sectional view and α symbolizes the ratio of filling. It should be noticed that instead of bending rigidity and mass density per unit length in Equation (1), solutions should be realized by writing the properties of the section to be examined (*E(r)I* and $\rho(r)A$ or $(EI)_{eq}$ and $(\rho A)_{eq}$). In order to reach the solution in the presented analytical method, modal displacement functions should be given as:

$$w(x,t) = v(x)\cos(\omega t)\,. \tag{8}$$

In this equation, ω represents the natural frequency and *v(x)* is the function of modal displacement, respectively. After determining the relations between the boundary points, the following modal displacement function is defined [25, 39]:

$$v(x) = \begin{bmatrix} \Psi_0 & x = 0 \\ \Psi_L & x = L \\ \sum_{j=1}^{\infty} D_j \sin(\alpha_j x) & 0 < x < L \end{bmatrix} \tag{9}$$

where in:

$$\alpha_j = \frac{j\pi}{L} \tag{10}$$

where L describes the column's length. The Fourier coefficient in Equation (9), D_j, can be obtained as follows:

$$D_j = \frac{2}{L}\int_0^L v(x)\sin(\alpha_j x)\partial x\,. \tag{11}$$

Equation (9) can be redefined as follows to satisfy the conditions:

$$v'(x) = \sum_{k=1}^{\infty} \alpha_j D_j \cos(\alpha_j x)\,. \tag{12}$$

Fourier cosine series should be used to redefine Equation (12)

$$v'(x) = \frac{r_o}{L} + \sum_{j=1}^{\infty} r_j \cos(\alpha_j x)\,. \tag{13}$$

The Fourier coefficients in Equation (13) are obtained as follows:

$$r_o = \frac{2}{L}\int_0^L v'(x)\partial x = \frac{2}{L}[v(L) - v(0)] \tag{14}$$

$$r_j = \frac{2}{L}\int_0^L v'(x)\cos(\alpha_j x)\partial x, (j = 1, 2...)\,. \tag{15}$$

The following results are obtained when the partial integrals are calculated:

$$r_j = \frac{2}{L}[v(x)\cos(\alpha_j x)] + \frac{2}{L}[\alpha_j \int_0^L v(x)\sin(\alpha_j x)]\partial x \tag{16}$$

$$r_j = \frac{2}{L}[(-1)^j v(L) - v(0)] + \alpha_j D_j\,. \tag{17}$$

The first derivative of the function is as given below:

$$\frac{dv(x)}{dx} = \frac{\psi_L - \psi_0}{L} + \sum_{j=1}^{\infty}\cos(\alpha_j x)(\frac{2((-1)^j\psi_L - \psi_0)}{L} + \alpha_j D_j)\,. \tag{18}$$

In this study, the water tank and the column are handled separately. In Equation (9), the tank part and the built-in support part in the foundation are defined as separate points. The continuous column part is expressed by the Fourier-Sine series. Using the procedure above, higher order equivalents of *v(x)* can be derived separately [25, 39]

$$\frac{d^2v(x)}{dx^2} = -\sum_{j=1}^{\infty}\alpha_j \sin(\alpha_j x)(\frac{2((-1)^j\psi_L - \psi_0)}{L} + \alpha_j D_j) \tag{19}$$

$$\frac{d^3v(x)}{dx^3} = \frac{\psi_L{}'' - \psi_0{}''}{L} + \sum_{j=1}^{\infty}\cos(\alpha_j x)(\frac{2((-1)^j\psi_L{}'' - \psi_0{}''}{L} - \alpha_j^2\frac{2((-1)^j\psi_L - \psi_0)}{L} + \alpha_j D_j) \tag{20}$$

$$\frac{d^4v(x)}{dx^4} = -\sum_{j=1}^{\infty}\alpha_j \sin(\alpha_j x)(\frac{2((-1)^j\psi_L{}'' - \psi_0{}'')}{L} - \alpha_j^2\frac{2((-1)^j\psi_L - \psi_0)}{L} + \alpha_j D_j)\,. \tag{21}$$

When Equations (19) and (21) are used instead of expressions in Equation (1):

$$\sum_{j=1}^{\infty}(\frac{2}{L}\cos(\omega t)\sin(\alpha_j x)(-LD_j(\rho(r)A\omega^2 - E(r)I\alpha_j^4) - 2\alpha_j((-1)^j(\psi_L(-E(r)I\alpha_j^2) + E(r)I\psi_L{}'') + \psi_0(E(r)I\alpha_j^2) + E(r)I\psi_L{}'' = 0\,. \tag{22}$$

Equation (22) has been written for a column with porosity, including the Fourier coefficient. Equation (23) may be expressed as follows in terms of ψ_0, ψ_L, ψ_0" and ψ_L":

$$D_j = \frac{2(\omega^2)_j}{-(\omega^2)_j + \omega^2}((\psi_0" - (-1)^j \psi_L") - \alpha_j^2(\psi_0 - (-1)^j \psi_L)). \tag{23}$$

The free vibration of a column with free support at both ends is represented by a function *v(x,t)*.

$$w(x,t) = \sum_{j=1}^{\infty} \frac{2(\omega^2)_j}{-(\omega^2)_j + \omega^2}((\psi_0" - (-1)^j \psi_L") - \alpha_j^2(\psi_0 - (-1)^j \psi_L))\cos(\omega t)\sin(\alpha_j x). \tag{24}$$

This function is applicable to all boundary conditions and is a more general and applicable version of existing techniques.

2.2. Defined Boundaries

Within the scope of this study, it is assumed that there is a mass at the structure's free end whose movement will be examined, and a column with a fixed support at the other end. These boundary conditions mentioned for the porous column are expressed mathematically as

$$\psi_0 = 0, \frac{\partial v(x,t)}{\partial x} = 0, x = 0 \tag{25}$$

$$\psi_L" = 0, \;\; k\psi_L - M\frac{\partial^2 v(x,t)}{\partial t^2} = EI\frac{\partial^3 v(x,t)}{\partial x^3}, \;\; x = L. \tag{26}$$

Here, k and M denote a spring and load attached to the end of the column, respectively. Substituting the expressions obtained in Equations (18), (20) and (23) at the corresponding places in Equations (25) and (26) yields two simultaneous homogeneous equations

$$(1 + \sum_{j=1}^{\infty} \frac{2\lambda^4(-1)^j}{\lambda^4 - j^4})\psi_L + (K - m\pi^2\lambda^4 + \sum_{j=1}^{\infty} \frac{2\lambda^4(-1)^j}{\lambda^4 - j^4})\psi_0" = 0 \tag{27}$$

$$(\sum_{j=1}^{\infty} \frac{2j^2}{\pi^2(\lambda^4 - j^4)})\psi_L + (1 + \sum_{j=1}^{\infty} \frac{2\lambda^4(-1)^j}{\lambda^4 - j^4})\psi_0" = 0 \tag{28}$$

where, Equations (27) and (28) can be represented in matrix form as:

$$\begin{bmatrix} \phi_{11} & \phi_{12} \\ \phi_{21} & \phi_{22} \end{bmatrix} \begin{bmatrix} \psi_L \\ \psi_0" \end{bmatrix} = 0 \tag{29}$$

where in

$$\phi_{11} = 1 + \sum_{j=1}^{\infty} \frac{2\lambda^4(-1)^j}{\lambda^4 - j^4} \tag{30}$$

$$\phi_{12} = K - m\pi^4\lambda^4 + \sum_{j=1}^{\infty} \frac{2\lambda^4\pi^2 j^2}{\lambda^4 - j^4} \tag{31}$$

$$\phi_{21} = \sum_{j=1}^{\infty} \frac{2j^2}{\pi^2(\lambda^4 - j^4)} \tag{32}$$

$$\phi_{22} = 1 + \sum_{j=1}^{\infty} \frac{2\lambda^4(-1)^j}{\lambda^4 - j^4}\,. \tag{33}$$

The relation given in Equation (29) is presented as the equation of an eigenvalue problem. If the determinant of the provided coefficient matrix in Equation (29) is taken and the determinant equation is set to "0", the mentioned eigenvalues can be easily obtained

$$\begin{bmatrix} \phi_{11} & \phi_{12} \\ \phi_{21} & \phi_{22} \end{bmatrix} = 0\,. \tag{34}$$

The expressions given in above equations are as follows for porous column:

$$K = \frac{kL^3}{E(r)I} \tag{35}$$

$$\lambda^4 = \frac{\rho(r)AL^4\omega^2}{\pi^4 E(r)I}\,. \tag{36}$$

While λ^4 and *K* expressions for perforated column are given as:

$$K = \frac{kL^3}{(EI)_{eq}} \tag{37}$$

$$\lambda^4 = \frac{(\rho A)_{eq} L^4\omega^2}{\pi^4 (EI)_{eq}}\,. \tag{38}$$

Here, λ and K denote the transformed (dimensionless) forms of circular frequency and spring stiffness, respectively. Also, it should be noted here that *m* (dimensionless form of mass) is considered with as given by Kim and Kim [39]. By using different (K) and (m) values to be used for different boundary conditions, the determinant given above can be used to solve different problems.

3. THE RESEARCH FINDINGS AND DISCUSSION

In the following section, a comparison example is presented to validate the solution method. For this purpose, Table 1 is given. Table 1 shows the dimensionless vibrational frequencies in the first 3 modes of a classical cantilever beam. If the results are found by choosing K = 0 and m = 0 with the formulations presented in this study, it is clear that the vibrational frequencies of a classical cantilever beam will be obtained. Because by choosing K = 0 and m = 0, the spring parameter and mass are neglected, respectively. For this comparison study, the infinite series's first 60 terms are used. As may be seen, an acceptable convergence is achieved. It must be noted that using more terms results in greater convergence.

Table 1. *Corroboration of the presented approach with frequencies of cantilever beam (K=0, m=0)*

	Cantilever Beam	Present study ($\lambda x \pi$)
Mode 1	1.875	1.88781
Mode 2	4.694	4.72627
Mode 3	7.855	7.90917

In this part of the study, vibration behaviors of a steel liquid storage tank with porous and perforated columns (seen Figure 2) designed as a water tower are presented. It is considered that the model of the designed water tower consists of three different parts: circular column made of porous material (or column made of perforated material), steel liquid storage tank and spring. While the porous column (or perforated column) is fixed to the ground with a built-in support, the tank is supported by the spring (seen Figure 2). The outer material of porous column is assumed as steel and Young's modulus and mass density of steel are as follows: E_o=210 GPa, ρ_o=7750 kg/m^3. Length and radius of porous column are equivalent to 40 m and 0.9 m, respectively. The ratio of the inner property to the outer property of the column affects the porosity. The outer material qualities are supposed to be constant, whereas the inner mechanical characteristics are assumed to be changing. Thus, the effect of various porosity values on vibration of storage tank is examined. Vibrational frequencies of the porous column are get and examined with the various porosity values, mass of the storage tank and spring parameters. In this study, the vibrational frequencies of the storage tank with porous column are given in the following form: $\Omega^4 = \dfrac{\rho_o A \omega^2 L^4}{E_o I}$. In addition, the frequency characteristics of the storage tank are computed using the first 60 entries of the infinite series. The following are the material and geometrical qualities of the perforated column: Young's modulus E=210 GPa, mass density ρ=7750 kg/m^3, length L=40 m. Perforated column dimensions are equal in width and thickness and 1.6 m is chosen. Thus, almost the same cross-sectional area with the porous column is selected and a better comparison is achieved between both column types. For perforated column, the vibrational frequencies are given in the following form: $\Omega^4 = \dfrac{\rho A \omega^2 L^4}{EI}$.

In Figure 3, variation of the ρ(r) / ρ_o of porous column is plotted for various e_2 values changing from 0 to 0.8. As can be understood from the figure, if e_2 is set to 0, the mass density properties of the column reflect the non-porous case. With increasing porosity values, this ratio *(ρ(r) / ρ_o)* falls below 1, that is, a decrease in the mass density of the column occurs.

In Figure 4, variation of the $(\rho A)_{eq} / \rho_o$ of perforated column is shown for various hole numbers (N) values changing from 1 to 10. Two deductions can be made easily from this Figure. First, increasing filling ratio increases the perforated column's equal mass each unit length. The second is that the equiv mass of each unit length of the column decreases with the increase in the number of holes.

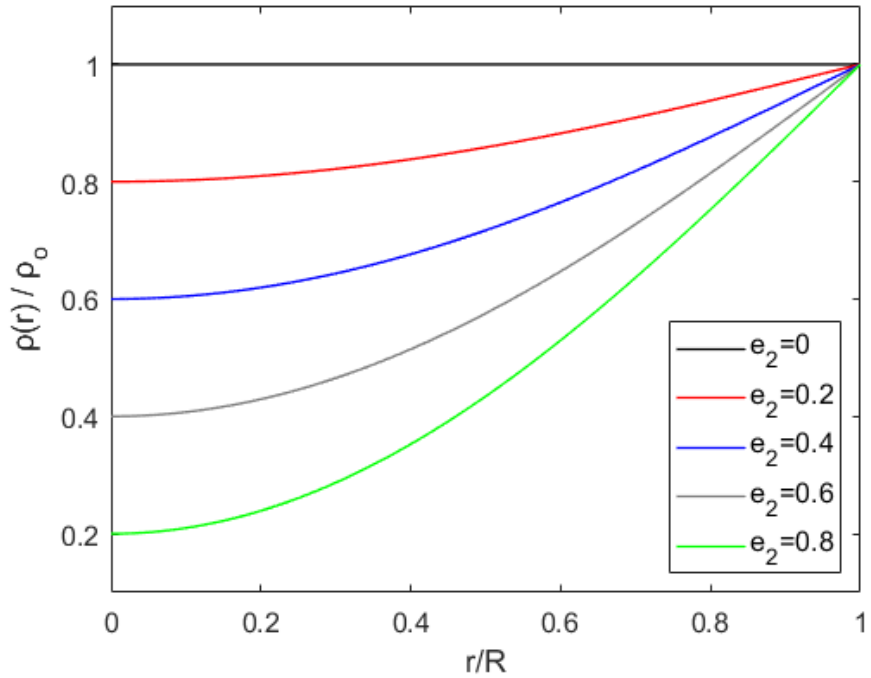

Figure 3. *The variability of $\rho(r)/\rho_o$ versus r/R for porous column*

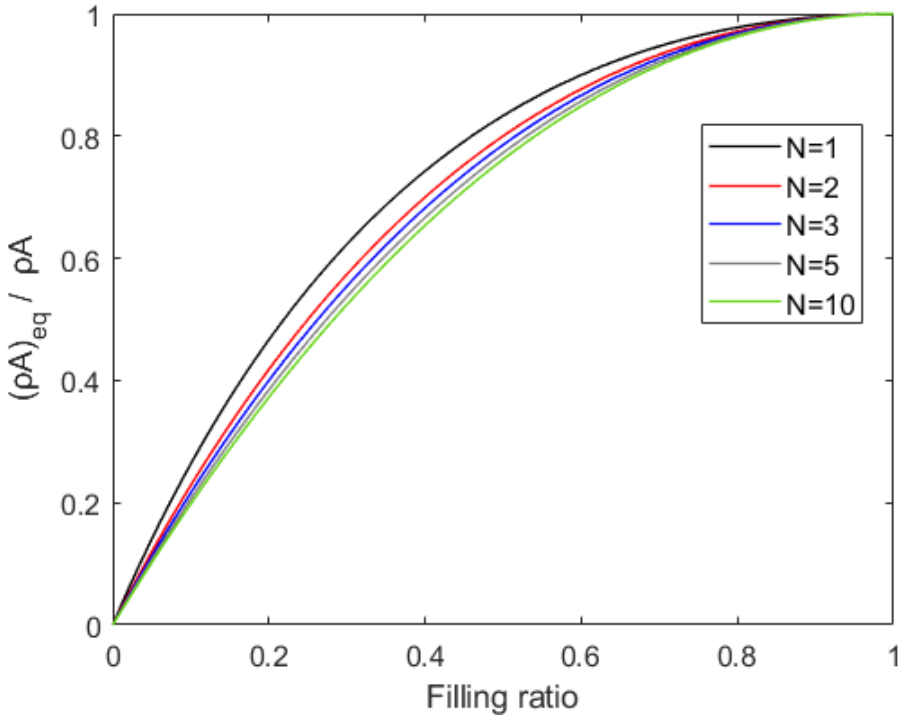

Figure 4. *The variation of $(\rho A)_{eq}/\rho A$ versus filling ratio for perforated column*

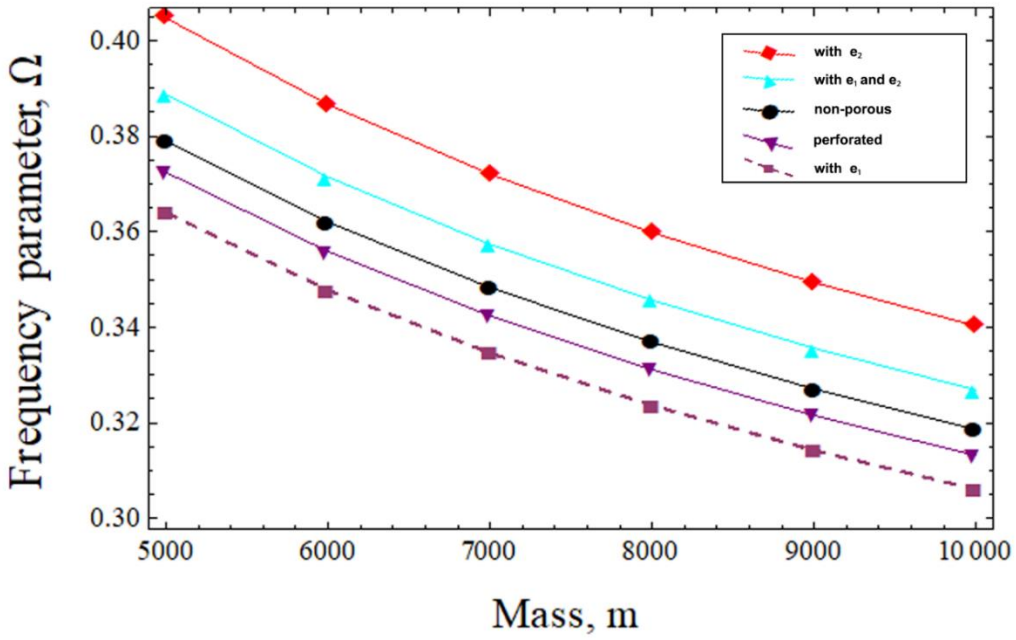

Figure 5. *The variation of the frequency parameter versus mass (K=100)*

In Figure 5, the variation of frequency parameter of storage tank is illustrated for various porosity, perforated or non-porosity conditions. For non-porosity condition, e_1 and e_2 are selected as zero (e_1=e_2=0). For the case where only e_1 is present, e_1 is set to 0.5 while e_2 is fixed to zero (e_1=0.5 & e_2=0). Similarly, in the case where only e_2 is examined, e_1 is set to zero, while e_2 is set to 0.5 (e_1=0 & e_2=0.5). When e_1 and e_2 affect the porous column at the same time, e_1=e_2=0.5 is set. And finally, N=4 and α=0.5 are selected for perforated column. Here, spring parameter K is selected as 100 and mass is ranging from 5000 to 10000. The impact of the mass on the frequency parameter of storage tank is investigated via Figure 5. Figure 5 clearly shows that increasing the mass induces a decrease in the frequency characteristics of the tank under all conditions.

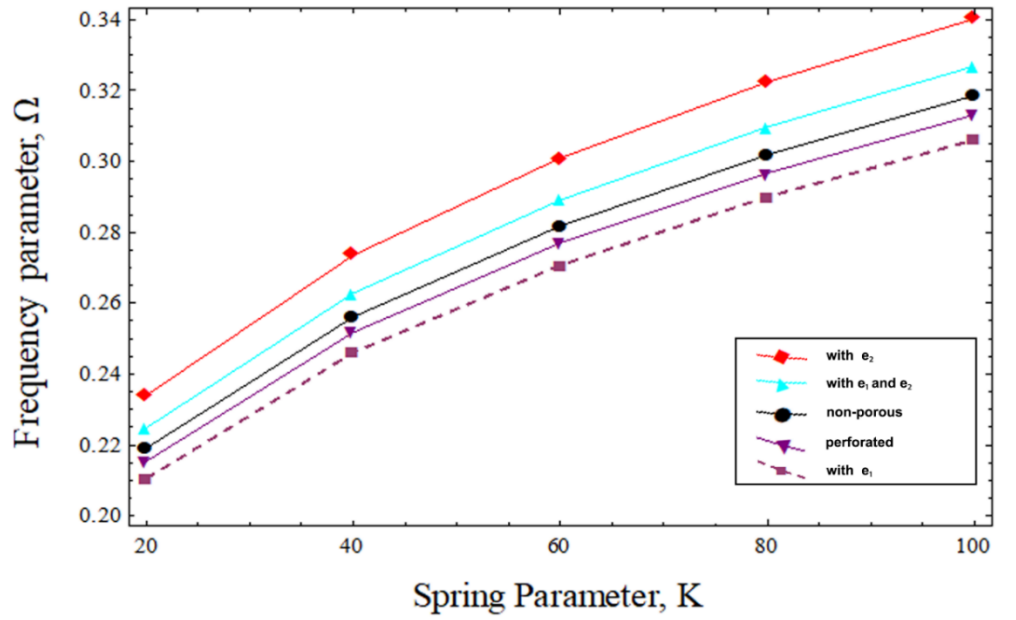

Figure 6. *The variety of the frequency parameter versus spring parameter (m=10000)*

To explain the influence of the spring parameter K, Figure 6 is plotted. For this aim, a variety of the frequency parameters versus spring parameters are investigated for the various porosity conditions

($e_1=e_2=0$, $e_1=0.5$ & $e_2=0$, $e_1=0$ & $e_2=0.5$, $e_1=e_2=0.5$) and perforated condition (N=4 & α=0.5). For this figure, the mass is equal to 10000. The figure shows that as the spring parameter is increased, the frequency parameter also increases. This reveals the hardening influence of the spring variable. In addition, Figure 5 and Figure 6 also explains the effects of pores and perforates on the frequency parameters of the liquid storage tank. As can be observed, the lowest frequency parameter numbers emerge when the column is considered only with e_1 porosity. In contrast, the highest parameter values of storage tank occur when only e_2 porosity is considered.

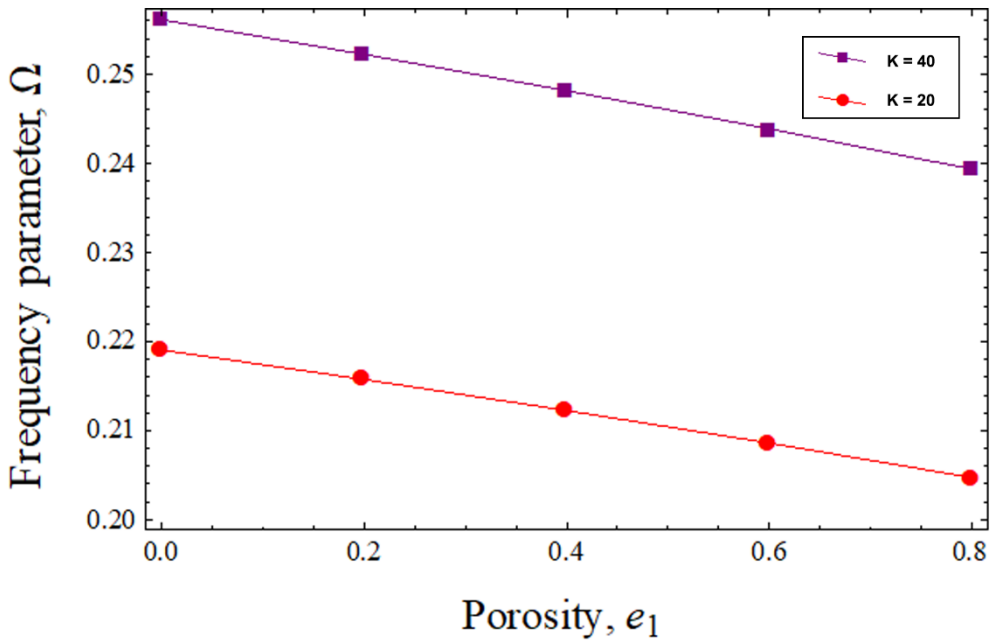

Figure 7. *The alteration of the frequency parameter versus porosity e_1 (m=10000)*

It is aimed to demonstrate the influence of the porosity e_1 via Figure 7. For this purpose, e_2 is set to zero, while e_1 values are changed from 0 to 0.8. It should be noted here that when e_1 is also zero, the liquid storage tank column exhibits the characteristics of a homogeneous column without porosity. In such a condition, the column behaves as a non-porous column made of steel. The reduction in frequency parameters with the rise in the e_1 porosity value is also evident in this figure. The reason for this is that increasing e_1 values create a drop in the storage tank column's Young's modulus.

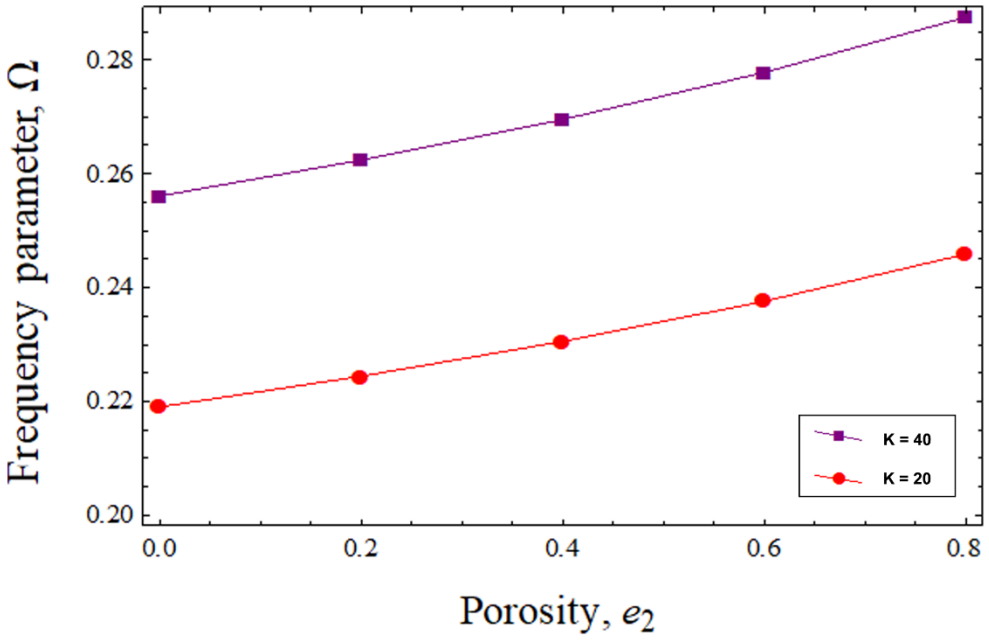

Figure 8. *The modification of the frequency parameter versus porosity e_2 (m=10000)*

Figure 8 is plotted to examine the effect of e_2 alone on storage tank vibration. For this investigation, e_1 is set to zero, while e_2 values are changed from 0 to 0.8. The increase in the frequency parameters of the storage tank with the increase in the e_2 porosity value can be seen obviously here also. Therefore, increasing e2 values leads the storage tank column's mass density to reduce. It is clear from here that increasing e_1 and e_2 have softening and hardening effects on the liquid storage tank, respectively. Also, Figures 7 and 8 can be used to refer once again to the hardening effect of the spring parameters.

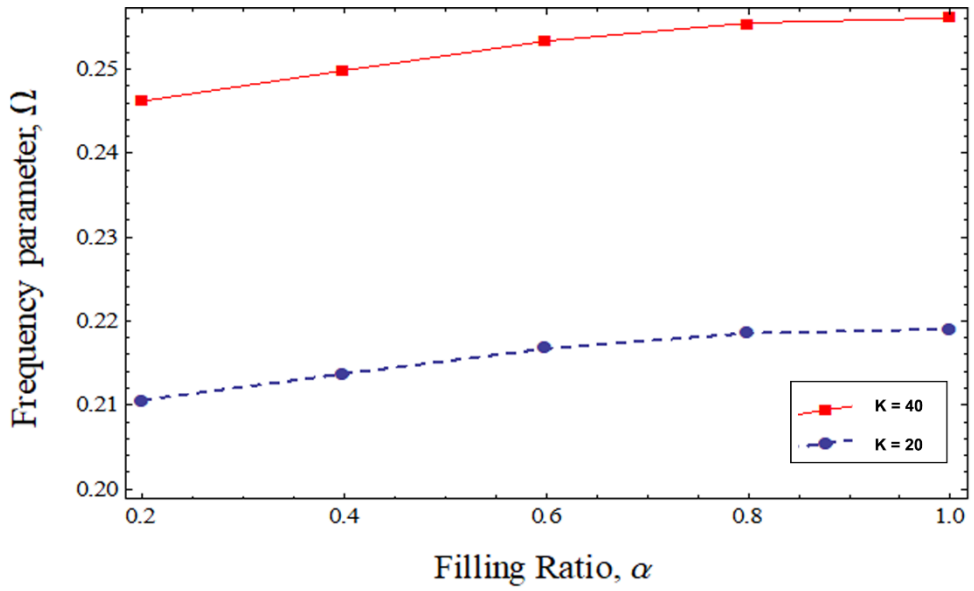

Figure 9. *The variation of the frequency parameter versus filling ratio α (m=10000)*

In Figure 9, it is intended to examine the effect of the filling ratio on the vibration of a perforated column storage reservoir. For this examination, N is set to 4, while filling ratio values are changed from 0.2 to 1. The increment in the frequency parameters of the liquid storage tank with the increase in the filling ratio value is observed here clearly. The reason for this is that increasing filling ratio values caused an increase in the Young's modulus of the storage tank perforated column. It is concluded from here that increasing filling ratio gives hardening effects on the liquid storage tank column.

Figure 10 is intended to show the impact of the number of holes. For this purpose, the filling ratio is set to 0.5, while hole numbers are changed from 2 to 10. The figure indicated that increasing the hole number generates a decrease in the frequency parameters. The reason for this is increasing hole numbers causes a decrease in the Young's modulus of the perforated column. As a consequence of this, it is concluded that increasing the number of holes has a softening effect on the liquid storage tank column.

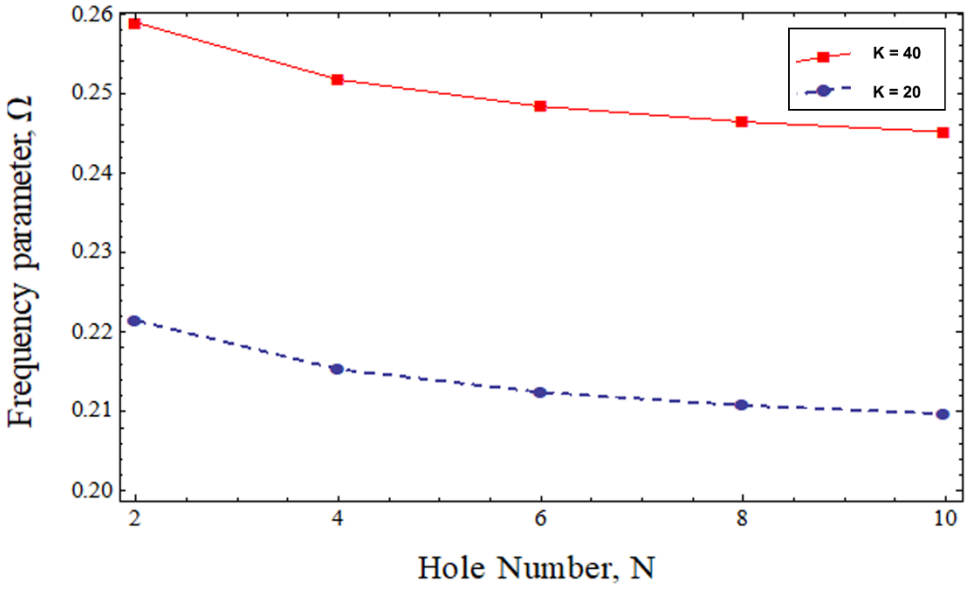

Figure 10. *The alteration of the frequency parameter versus number of holes N (m=10000)*

4. RESULTS

In the present study, an analytical solution based on the Euler-Bernoulli beam theory is presented to model the free vibration behavior of a liquid storage tank with porous and perforated columns. The effects of diverse parameters, for instance, number of holes N, filling ratio, porosity e_1, porosity e_2, spring parameter and mass parameter on the vibrational frequency parameters of the storage tank are studied via an exact continuum method. Some prominent results have been obtained: The mass of a liquid storage tank is well-known to play an important role in its vibration behavior, and this factor is also demonstrated in this study. It can be observed that increasing the mass produces a lowering in the tank's frequency characteristics. This decrement is valid for all column types (non-porous, porous and perforated) that have been examined in this work. In contrast to the effectiveness of the mass, the increase in terms of the spring parameter value has an enhancing effect on the frequencies. When the column is considered with e_1 porosity originating from the Young's modulus, it can be observed that the frequency parameters of the storage tank reduces. If the column is considered with e_2 porosity originating from the mass density, the frequency parameters of the storage tank increase. Considering the tank column as perforated, the effects of the number of holes and the filling ratio attract attention. The frequency values rise as the filling ratio increases. On the other hand, a rise in the number of holes causes a fall in the frequencies.

CONFLICTS OF INTEREST

No conflict of interest was declared by the authors.

REFERENCES

[1] Kirkland, J.J., "Techniques for High-Performance Liquid-Liquid and Ion Exchange Chromatography with Controlled Surface Porosity Column Packings", Journal of Chromatographic Science, 7(6): 361–365, (1969).

[2] Cabooter, D., Lynen, F., Sandra, P., Desmet, G., "Total pore blocking as an alternative method for the on-column determination of the external porosity of packed and monolithic reversed-phase columns", Journal of Chromatography A, 1157(1-2): 131–141, (2007).

[3] Alyousef, R., Alabduljabbar, H., Mohamed, A. M., Alaskar, A., Jermsittiparsert, K., Ho, L., "S. A model to develop the porosity of concrete as important mechanical property", Smart Structures and Systems, 26(2): 147–156, (2020).

[4] Huang, J., Alyousef, R., Suhatril, M., Baharom, S., Alabduljabbar, H., Alaskar, A., Assilzadeh, H., "Influence of porosity and cement grade on concrete mechanical properties", Advances in Concrete Construction, 10(5): 393–402, (2020).

[5] Bekkaye, T. H. L., Fahsi, B., Bousahla, A. A., Bourada, F., Tounsi, A., Benrahou, K. H., Al-Zahrani, M. M., "Porosity-dependent mechanical behaviors of FG plate using refined trigonometric shear deformation theory", Computers and Concrete, 26(5): 439–450, (2020).

[6] Roy, D. M., Gouda, G. R., "Porosity-Strength Relation in Cementitious Materials with Very High Strengths", Journal of the American Ceramic Society, 56(10): 549–550, (1973).

[7] Bachtiar, E., Tjaronge, M.W., Zulharnah, Irfan, U. R., "Porosity, Pore Size and Compressive Strength of Self Compacting Concrete Using Sea Water", Procedia Engineering, 125: 832-837, (2015).

[8] Kim, J. Y, Edil, T. B., Park, J. K., "Effective Porosity and Seepage Velocity in Column Tests on Compacted Clay", Journal of Geotechnical and Geoenvironmental Engineering, 123(12): 1135-1141, (1997).

[9] Dores-Sousa, J.L., Terryn, H., Eeltink, S., "Morphology optimization and assessment of the performance limits of high-porosity nanostructured polymer monolithic capillary columns for proteomics analysis", Analytica Chimica Acta, 1124: 176-183, (2020).

[10] Cunningham, R., Nicolas, A., Madsen, J., Fodran, E., Anagnostou, E., Sangid, M. D., Rollett, A. D., "Analyzing the effects of powder and post-processing on porosity and properties of electron beam melted Ti-6Al-4V", Materials Research Letters, 5(7): 516-525, (2017).

[11] Najafzadeh, M., Adeli, M. M., Zarezadeh, E., Hadi, A., "Torsional vibration of the porous nanotube with an arbitrary cross-section based on couple stress theory under magnetic field", Mechanics Based Design of Structures and Machines, 1-15, (2020).

[12] Zhao, C., Chen, J., Xu, Q., Wang, J., Wang, B., "Investigation on sloshing and vibration mitigation of water storage tank of AP1000", Annals of Nuclear Energy, 90: 331-342, 0306-4549, (2016).

[13] Kim, Y.-W., Lee, Y.-S., "Coupled vibration analysis of liquid-filled rigid cylindrical storage tank with an annular plate cover", Journal of Sound and Vibration, 279(1-2): 217–235, (2005).

[14] Cho, J. R., Lee, H. W., Kim, K. W., "Free Vibration Analysis of Baffled Liquid-Storage Tanks by The Structural-Acoustic Finite Element Formulation", Journal of Sound and Vibration", 258(5), 847–866, (2002).

[15] Tedesco, J. W., Kostem, C. N., Kalnins, A., "Free vibration analysis of cylindrical liquid storage tanks", Computers and Structures, 26(6): 957–964, (1987).

[16] Pina, C.G, Meirelles, A.J.A, "Deacidification of corn oil by solvent extraction in a perforated rotating disc column", Journal of the American Oil Chemists' Society, 77: 553-559, (2000).

[17] Tsavdaridis, K. D., Faghih, F., Nikitas, N., "Assessment of Perforated Steel Beam-to-Column Connections Subjected to Cyclic Loading", Journal of Earthquake Engineering, 18(8): 1302-1325, (2014).

[18] Liu, X., Yu, C., Xin, F., "Gradually perforated porous materials backed with Helmholtz resonant cavity for broadband low-frequency sound absorption", Composite Structures, 263: 113647, (2021).

[19] Abdelrahman, A. A., Eltaher, M. A., Kabeel, A. M., Abdraboh, A. M., Hendi, A. A. "Free and forced analysis of perforated beams", Steel and Composite Structures, 31(5): 489-502, (2019).

[20] Almitani, K. H., Abdelrahman, A. A., Eltaher, M. A. "Stability of perforated nanobeams incorporating surface energy effects", Steel and Composite Structures, 35(4): 555-566, (2020).

[21] Assie, A., Akbaş, Ş. D., Bashiri, A. H., Abdelrahman, A. A., Eltaher, M. A. "Vibration response of perforated thick beam under moving load", The European Physical Journal Plus, 136(3): 1-15, (2021).

[22] Hassannejad, R., Hosseini, S. A., Alizadeh-Hamidi, B., "Influence of non-circular cross section shapes on torsional vibration of a micro-rod based on modified couple stress theory", Acta Astronautica, 178: 805-812, (2021).

[23] Yaylı, M. Ö., Uzun, B., Deliktaş, B., "Buckling analysis of restrained nanobeams using strain gradient elasticity", Waves in Random and Complex Media, 1: 20, (2021).

[24] Uzun, B., Kafkas, U., Yaylı, M.Ö., "Stability analysis of restrained nanotubes placed in electromagnetic field", Microsystem Technologies, 26: 3725–3736, (2020).

[25] Yaylı, M.Ö., "Axial vibration analysis of a Rayleigh nanorod with deformable boundaries", Microsystem Technologies, 26(9): 3725–3736, (2020).

[26] Uzun, B., Civalek, Ö., Yaylı, M. Ö., "Vibration of FG nano-sized beams embedded in Winkler elastic foundation and with various boundary conditions", Mechanics Based Design of Structures and Machines, 1: 20, (2020).

[27] Abdelrahman, A. A., Esen, I., Özarpa, C., Shaltout, R., Eltaher, M. A., Assie, A. E., "Dynamics of perforated higher order nanobeams subject to moving load using the nonlocal strain gradient theory", Smart Structures and Systems, 28: 515-533, (2021).

[28] Jalaei, M., Civalek, O., "On dynamic instability of magnetically embedded viscoelastic porous FG nanobeam", International Journal of Engineering Science 143: 14-32, (2019).

[29] Akbas, S. D, Ersoy, H., Akgöz, B., Civalek, O., "Dynamic Analysis of a Fiber-Reinforced Composite Beam under a Moving Load by the Ritz Method", Mathematics, 9: 1048, (2021).

[30] Numanoğlu, H.M., Akgöz, B., Civalek, O., "On dynamic analysis of nanorods", International Journal of Engineering Science 130: 33-50, (2018).

[31] Akgöz, B., Civalek, O., "Longitudinal vibration analysis for microbars based on strain gradient elasticity theory", Journal of Vibration and Control 20(4): 606-616, (2014).

[32] Civalek, O., Uzun, B., Yaylı, M.O., Akgöz, B., "Size-dependent transverse and longitudinal vibrations of embedded carbon and silica carbide nanotubes by nonlocal finite element method", The European Physical Journal Plus , 135: 356-381, (2020).

[33] Civalek, Ö., Numanoğlu, H. M., "Nonlocal finite element analysis for axial vibration of embedded love–bishop nanorods", International Journal of Mechanical Sciences, 188: 105939, (2020).

[34] Uzun, B., Yaylı, M. Ö., Deliktaş, B., "Free vibration of FG nanobeam using a finite-element method", Micro and Nano Letters, 15(1): 35-40, (2020).

[35] Uzun, B., Kafkas, U., Yaylı, M. Ö., "Free vibration analysis of nanotube based sensors including rotary inertia based on the Rayleigh beam and modified couple stress theories", Microsystem Technologies, 27(5): 1913-1923, (2021).

[36] Karabulut, H., Ersoy, H., "Dynamic behaviors of a Two-cylinder Four-Stroke", Gazi University Journal of Science, 25(2): 519-532, (2012).

[37] İpci, D., Yıldırım, B., "Free Vibration Analysis of a Functionally Graded Micro-Beam with Tapered Cross Section", Gazi University Journal of Science Part C: Design and Technology, 9(2): 272-282, (2021).

[38] Reddy, J.N., "Nonlocal theories for bending, buckling and vibration of beams", International Journal of Engineering Science, Sci. 45: 288-307, (2007).

[39] Kim, H. K., Kim, M. S., "Vibration of beams with generally restrained boundary conditions using Fourier series", Journal of Sound and Vibration, 245(5), 771-784, (2001).